HHS Public Access

Author manuscript

Mater Sci Eng C Mater Biol Appl. Author manuscript; available in PMC 2021 February 01.

Published in final edited form as:

Mater Sci Eng C Mater Biol Appl. 2020 February ; 107: 110311. doi:10.1016/j.msec.2019.110311.

Wavy Small-Diameter Vascular Graft Made of Eggshell Membrane and Thermoplastic Polyurethane

Shujie Yan[a,b,c,d], **Brett Napiwocki**[d], **Yiyang Xu**[a,b,c,d], **Jue Zhang**[e], **Xiang Zhang**[a,b], **Xiaofeng Wang**[a,b], **Wendy C. Crone**[d], **Qian Li**[a,b,*], **Lih-Sheng Turng**[c,d,*]

[a]School of Mechanics and Engineering Science, Zhengzhou University, Zhengzhou, China

[b]National Center for International Research of Micro-Nano Molding Technology Zhengzhou University, Zhengzhou, China

[c]Polymer Engineering Center, Department of Mechanical Engineering University of Wisconsin–Madison, Madison, WI, USA

[d]Wisconsin Institute for Discovery University of Wisconsin–Madison, Madison, WI, USA

[e]Morgridge Institute for Research, Madison, WI, USA

Abstract

In this study, a small-diameter, double-layered eggshell membrane/thermoplastic polyurethane (ESM/TPU) vascular graft with a wavy structure was developed. The avian eggshell membrane, a fibrous structure similar to the extracellular matrix (ECM), has the potential to yield rapid endothelialization *in vitro*. The dopamine and heparin modification of the ESM surface not only promoted human umbilical vein endothelial cell (HUVEC) proliferation via cytocompatibility assessment, but also improved its anticoagulation properties as verified in platelet adhesion tests. The biomimetic mechanical properties of the vascular graft were provided by the elastic TPU fibers via electrospinning using a wavy cross-section rotating collector. The advantage of combining these two materials is to make use of the bioactivity of ESM as the internal membrane and the tunable mechanical properties of TPU as the external layer. The circumferentially wavy structure of the vascular graft produced a toe region in the non-linear section of the stress–strain curve similar to that of natural blood vessels. The ESM/TPU graft's circumferential ultimate strength was 2.57 MPa, its strain was 339% mm/mm, and its toe region was found to be around 20% mm/mm. Cyclical tension tests showed that the vascular graft could maintain good mechanical properties and showed no structural damage under repeated extension tests.

[*]**Corresponding authors:** Lih-Sheng Turng, Tel: 608-316-4310; turng@engr.wisc.edu, Qian Li, Tel: +86-371-67781750; qianli@zzu.edu.cn.

Disclosure statement

Declarations of interest: none.

Keywords

Eggshell membrane; thermoplastic polyurethane; endothelialization; antithrombogenicity; small-diameter vascular graft

1. Introduction

Cardiovascular disease (CVD) is the number one cause of death worldwide [1,2]. Nowadays, almost 17.3 million adults suffer from CVD every year [3]. Costs associated with CVD have risen to almost 17% of overall national health expenditures in the United States alone [4,5]. Blood vessel replacement surgeries are commonly used to replace diseased blood vessels [6,7]. Autografts undoubtedly have the best biocompatibility and will not cause rejection. However, autografts, even if available, have some disadvantages, including secondary trauma, pain, infection, and slow healing at donor sites. Allografts, which refer to human donor tissues, also bring hope to the shortage of human transplant vessels. Scientists try to ensure that the cells in the allografts are compatible with the patient's blood. However, cryopreservation to preserve tissue organism activity and function of allogeneic blood vessels has yet to be accomplished. Furthermore, allograft rejection can occur, resulting in an undesirable immune system response and rejection [8,9]. For medium- to large-diameter blood vessels, artificial vascular grafts, including expanded polytetrafluoroethylene (ePTFE), Dacron, nylon [10,11], and polyurethane (PU) [12,13], have been developed and used in clinical operation [14,15]. Artificial vascular grafts provide good and long-term patency for vessels with an inner diameter (ID) larger than 6 mm, but fail fairly quickly for vessels with an ID of less than 6 mm. The blood in small diameter vessels flows slowly, and clots can easily form on their luminal surface and cause thrombosis [16].

In order to improve the patency of small diameter vascular grafts, a procedure for endothelialization on the eggshell membrane/thermoplastic polyurethane (ESM/TPU) vascular graft has been developed in this study. The luminal surface of the TPU graft was combined with ESM to allow for the seeding of endothelial cells. ESM is the part of an egg that is generally considered waste. However, ESM's fibrous structure and excellent biocompatibility have attracted wide interest [17–19]. Natural biomaterial ESM, composed of keratin biofiber, helps air exchange while preventing bacteria from reaching the inside of the egg [20,21]. It is a unique bi-layered biomaterial comprised of abundant collagens, 18 kinds of amino acids, elastin, glucosamine, hyaluronic acid, and chondroitin [22,23]. ESM has found wide application in tissue engineering. Maeda et al. used ESM as a surgical dressing for burns because it helps skin and wounds to heal [24,25]. Arias et al. used ESM as a biodegradable bone regeneration inhibitor [26]. Ohto–Fujita et al. discovered that hydrolyzed ESM could provide an extracellular matrix environment for human dermal fibroblast cells [27]. Balaz and Jia found that ESM guided tissue regeneration [28,29]. It has also been commercialized into other health products [30,31]. ESM has a similar function as the human amniotic membrane for protecting the fetus. Its suitability for the adhesion and growth of endothelial cells will be explored in this study.

Thermoplastic polyurethane (Tecoflex TPU SG-93A) is a multi-block linear polymer. It has very good elasticity, flexibility, and high mechanical strength. It is a hyperelastic material that can with- stand repeated stress just like a native blood vessel being subjected to the flow of blood. TPU has wide application in the biomedical field [32]. Therefore, TPU and ESM were chosen as the constituent materials to fabricate double-layer, small-diameter, artificial vessels.

Because current small-diameter artificial vascular grafts easily cause thrombosis, to obtain long-term patency with small-diameter vascular grafts, rapid endothelialization of the luminal surface and good mechanical properties are necessary [33–36]. This research aimed to design patent small-diameter vascular grafts by utilizing ESM to promote endothelial cell proliferation to mimic the vascular intima surface, and by creating a wavy structure using TPU to reproduce the mechanical behavior of natural blood vessels. The wavy small-diameter ESM/TPU vessel grafts have great significance for further application.

2. Experimental Methods

2.1. Materials

Raw chicken ESM clings to the shell closely, so acid soaking is required to separate it from the eggshell. Once this occurs, the ESM can be easily obtained by manually peeling it from the eggshell. The ESM was rinsed with DI water to remove any residual acid before using. Medical-grade thermoplastic polyurethane (TPU) pellets, Tecoflex™ SG-93A (hardness: 87A), were provided by Lubrizol. N,n-dimethyl formamide (DMF), heparin sodium salt from porcine intestinal mucosa (CAS Number 9041081), Toluidine Blue O, and dopamine hydrochloride were all purchased from Sigma- Aldrich. The capacity of heparin and its rate of release on the H-PDA-ESM were tested by Toluidine Blue O assay [37]. The heparin on the sample was about 50 $\mu g/cm^2$, and the rate of release of the heparin was about 60% for 10 days (Supporting Information, Fig. S1).

2.2. TPU Electrospinning

Electrospinning is a commonly used, conventional technique for preparing tissue engineering grafts. In this study, TPU pellets were dissolved in a DMF solution to obtain a 10 w/v% concentration. The solution was then stirred at 50 °C overnight before electrospinning. A syringe pump (Harvard Apparatus 11 Plus) was used to control the electrospinning rate at 0.5 ml/h with a metal needle diameter of 1.2 mm. The electrospinning positive voltage was 20 kV, the ambient humidity was 32–38%, and the needle–rotator distance was 18 cm [38]. The TPU electrospinning time was 16 hours for an 8 ml solution, and a wavy cross-section tubular collector was used in the process.

2.3. Eggshell Membrane Modification

To investigate the effect of modified ESM on cell behavior, the ESM was treated with dopamine (DA) and heparin. First, a tris(hydroxymethyl) aminomethane solution was prepared (10 mM, pH 8.5) as a buffer to dissolve the dopamine. Then ESMs were immersed in 2 ml/ml of a dopamine solution overnight at room temperature. The pyrocatechol group of dopamine was oxidized to yield benzoquinone in air. Then, pyrocatechol and benzoquinone

produced a disproportionation reaction and formed a cross bond [39]. The dopamine was polymerized under weak alkalinity. Then, polydopamine (PDA) was able to be coated on the ESM surface due to its strong adhesive properties [40][41]. The polydopamine-modified ESMs were named PDA-ESM.

To further enhance the antithrombogenic properties, heparin was chemically grafted onto the surface of the PDA-ESM. A heparin solution (1 mg/mL) was prepared using the above-mentioned buffer. The polydopamine-coated ESMs were immersed into the heparin solution at 4 °C for 12 h, which was enough time for the heparin and polydopamine to covalently bond. The resulting heparin-immobilized PDA-ESMs were named H-PDA-ESM. The heparin was also grafted on the neat ESM for comparison using the same method; these samples were named H-ESM. Polydopamine enhanced the combination between ESM and heparin, and heparin was used to inhibit platelet adhesion to prevent the formation of thrombi.

2.4. Mechanical Properties

Natural blood vessels have unique mechanical properties due to their wavy elastin and collagen fibers in the vessel walls [42]. To obtain natural blood vessel mechanical properties, the vascular grafts were designed with a wavy structure. A metal tubular collector with a wavy cross-section was used in the electrospinning process. Thus, after removing the double-layered TPU/ESM graft from the mandrel, a wavy structure was obtained. The circumferential tensile test curve shows three stages: the toe region, linear region, and yield and failure region. In the toe region, curly elastin fibers unfold under low stress and show large strain. This region is responsible for the nonlinear stress–strain curve because the slope of the toe region is different from that of the linear region. With the strain increasing, collagen fibers stretch and extend—this is the linear stage where strain increases sharply [43–45].

Tensile tests were carried out on a universal mechanical testing machine (Instron 5967) at room temperature (23 °C). Samples remained in hydrated condition. The samples were immersed in water until the start of the tests. As the tests ended very quickly, a regular chamber was used to prevent water evaporation. Circumferential tensile tests were conducted for grafts using a 30 KN load cell. The samples were tubular shaped, with a tube diameter of 4 cm. The tube samples were cut 1 cm in length and held with two L-shaped grips. The tensile test specimens were stretched in the radial direction at a speed of 5 mm/min until the sample broke.

Circumferential cyclical stretches were performed using the same method. A constant elongation rate of 100 mm/min was set and the sample was stretched to 50% strain, and then released to 0% strain, repetitively, for 100 cycles.

2.5. General Characterization of Prepared Grafts

2.5.1 SEM—The ESM inner and outer surfaces, as well as the TPU surface and the double-layered cross-section morphological properties of the grafts, were characterized by scanning electron microscopy (SEM). The grafts were sputter-coated with a 10 nm thick

layer of platinum and pictures were taken using a NeoScope JCM-5000 SEM at a voltage of 10 kV.

2.5.2 FTIR—To verify the modifications to the ESM surface, including the original ESM, PDA-ESM, H-ESM, and H-PDA-ESM, Fourier transform infrared (FTIR) spectra (Bruker Tensor 27) were tested in the range of 4000–600 cm^{-1} at a resolution of 4 cm^{-1} using the attenuated total reflection (ATR) method.

2.6. In Vitro Cytocompatibility Assessment with Human Umbilical Vein Endothelial Cells (HUVECs)

In this study, human umbilical vein endothelial cells (HUVECs) were purchased from Lonza. HUVECs were used for cell viability testing to assess the feasibility of ESM/TPU membranes for biological applications. Cells were cultured on T75 flasks and fed every day using an EGM-2 bullet kit medium (Lonza). The culture was performed in a thermostatic incubator at 37 °C in a 5% CO_2 and 95% air environment. At confluence, HUVECs were dissociated with TrypLE Express enzyme (Gibco) to obtain suspended cells, centrifuged, and resuspended in medium prior to cell seeding.

Morphology, adhesion, and proliferation of HUVECs on ESM/TPU grafts were evaluated by phalloidin/DAPI staining, live and dead assay, and CCK-8 assay. The specimens had a round shape with a 15.6 mm diameter that fit in a 24-well culture plate. The shell side surfaces of the original ESM, PDA-ESM, H-ESM, H-PDA-ESM, and TPU surfaces were all used for cell seeding for cytoompatibility tests with tissue culture plates (TCPs) as the control. The number of replicates was four.

Prior to cell seeding, the graft samples were cut into sections of the same circular dimensions, put in 24-well TCPs, and washed using 70% ethanol, followed by washing three times with phosphate-buffered saline (PBS). Each side was also subjected to 30 min of ultraviolet sterilization (the lamp power was 6 W and the distance between the lamp and the sample was 50 cm). All samples were seeded with enzymatically detached HUVECs at a density of 2×10^4 cells/cm^2, and TCPs were planted with the same number of cells as the control. The medium was replaced daily.

To further confirm live and dead cells, fluorescence staining was performed on chosen samples using a live/dead viability/cytotoxicity kit (Life Technologies). Cell viability was determined after culturing for 1, 3, and 7 days. A kit containing green fluorescent calcein-AM and red fluorescence ethidium homodimer-1 (EthD-1) was used to stain both live and dead cells simultaneously. The samples were immersed in a staining solution (300 μl/cm^2) away from light for 20 min at 24 °C and then imaged by a Nikon fluorescence microscope.

Cell proliferation was assessed on day 1, 3, and 7 by CCK-8 assay using a Cell Counting Kit-8 (Dojindo Molecular Technologies). The samples were incubated in colorless medium with 10% CCK-8 solution away from light for 2 h. After incubation, the spent media containing formazan was transferred into a clear 96-well plate. A Glomax-Multi multiplate reader (Promega) was used to test the absorbance of formazan at the 450 nm wavelength to compare cell proliferation. The medium used in the CCK-8 assay was colorless to avoid the

effects of the medium's color. The CCK-8 solution was added to a blank well as a control. The final results were the sample test results minus the control result.

4′,6-diamidino-2-phenylindole (DAPI, Sigma-Aldrich) and phalloidin fluorescent staining (Biotium) were used for marking the cell nuclei and cytoskeleton f-actin molecules, respectively, to visualize the HUVECs morphology on the samples. The samples with HUVECs were washed three times, then fixed with 4% paraformaldehyde in PBS for 15 minutes on ice, followed by a PBS rinse, and then penetrated with 0.5% Triton X-100 in PBS for 10 min. Next, red fluorescent phalloidin solution stained the cell cytoskeleton for 20 min and blue fluorescent DAPI solution stained the cell nuclei for 5 min, both away from light and at room temperature. The staining process followed the manufacturer's recommendations. Images were captured at day 7 using the same fluorescence microscope.

The interaction between the cells and the substrate was observed using SEM. The samples stained with phalloidin/DAPI were gradient dehydrated with an alcohol solution using a series of concentrations (50, 60, 70, 80, 90, and 100%) for 15 min each and then sufficiently dried in a freeze dryer. The samples were then sputter coated with platinum and observed by SEM.

2.7. Platelet Adhesion Test

A platelet adhesion assay was performed to evaluate the effect of surface modification on the risk of thrombosis. The original ESM, PDA-ESM, H-ESM, H-PDA-ESM, and TPU samples were used in the platelet adhesion tests and the TPU sample was used as the control. Single-donor human whole blood was purchased from Innovative Research. The blood was added into the centrifuge tube, followed by centrifuging at 2000 rpm for 10 min, to obtain platelet-rich plasma (PRP). Before the platelet adhesion test, the samples were washed with PBS and added into the 24-well plate. Then, 200 μL of PRP were added to each sample and incubated at 37 °C for 2 h. After incubation, the samples were rinsed three times with PBS and adsorbed platelets were fixed with 2.5 wt% glutaraldehyde at 4 °C overnight. Then the samples were dehydrated with different concentrations of alcohol (50, 60, 70, 80, 90, and 100%) for 15 min each and sufficiently dried in a freeze dryer, followed by platinum coating and imaging using SEM.

2.8. Preparation of ESM/TPU Grafts

In this study, a small-diameter vessel with a double-layer, circumferentially wavy structure was designed. The electrospinning fibers were collected on a rotating collector with a wavy cross-section, without any post-processing. The encapsulation of ESM was carried out using electrospun TPU nanofibers (435.86 ± 173.27 nm). In Fig. 1, the original ESM was used as the endothelial cell (EC) basement membrane. The ESM was rolled on a customized, wavy mandrel, and then the mandrel was used as the rotating collector in the electrospinning process. A layer of TPU nanofibers was then electrospun and collected on the outside of the ESM to be used as the vascular outer layer. Specifically, an ultrathin layer of poly(ethylene oxide) (PEO) solution was coated on the outside of the ESM to enhance its combination with the TPU electrospinning fibers. After the eggshell membrane and the TPU were

collected on the mandrel, the wavy structure was copied onto the inner surfaces of the resulting blood vessel grafts.

3. Results and Discussion

3.1. Morphology of ESM/TPU Grafts

Figure 2 (A) and (B) exhibit the appearance and cross-section of a double-layer artificial vessel made of ESM and surrounded by an electrospun TPU layer. The double-layered cross-section morphological properties of the grafts were characterized by scanning electron microscopy (SEM) (cf. Fig. 2 (C) and (D). The inner and outer diameters of this graft were about 4 mm and 6 mm, respectively, and the wavy profile could be seen clearly. The compact layer between the ESM and TPU was a PEO coating that enhanced the combination of the two layers; it is shown in Fig. 2 (E) and (F).

Scanning electron microscopy (SEM) images of the electrospun TPU fibers and the ESM shell side and white side morphologies and substructures are shown in Fig. 3. The TPU membrane shows a porous structure from the side view and the fibers are uniform and continuous, with diameters mostly ranging from 200 to 600 nm.

Upon further inspection, the inner surface of the graft presents a fibrous network, which is the ESM's eggshell side. Because the ESM's inner and outer surfaces have different morphologies, it's important to identify the sides of the two layers. The ESM close to the shell side showed a fibrous structure similar to electrospun fibers, and the fiber diameters were 2244 ± 531 nm. These fiber sizes were suitable for blood vessel graft [46]. The ESM close to the white side showed numerous rounded bulges. The thickness of the ESM layer was about 50–70 μm [47,48]. Here, ESM's eggshell side was used as the graft's luminal side, meaning that it was in contact with the mandrel. The numerous bulges on the egg white side of the ESM promoted bonding with the TPU membrane. The TPU pore size was about 5.29 μm ± 1.71 μm, while the ESM pore size was about 8.78 μm ± 2.6 μm (Supporting Information, Fig. S2).

Figure 4 shows the cross-section of the vessel in the axial direction. The ESM and TPU layers can be seen to have bonded closely together. The ESM and TPU fibrous structures successfully mimicked the extracellular matrix.

3.2. Mechanical Properties

The outer TPU layer fabricated by electrospinning displayed a fibrous morphology that supported the ESM and was used to provide the vessels with the desired mechanical properties. The circumferentially wavy structure allowed for a greater radial expansion with a small circumferential stress, resulting in the typical toe region of natural blood vessels during the circumferential tensile test, thereby successfully mimicking the nonlinear mechanical behavior of natural blood vessels. The toe region, which started at the beginning of the stress–strain curve, has been marked with a blue box in Fig. 5 (A). Figure 5 (B) shows the amplified toe region.

As can be seen in Fig. 5, TPU has very good tensile strength, which enhances the mechanical properties of the double-layer ESM/TPU grafts. From referenced reports, human blood vessels have a circumferential tensile strength of 0.8 to 3.3 MPa and a tensile strain of 49–105%. The human coronary artery toe region is between 18 and 38% [49,50]. In Fig. 5 A, the ESM/TPU graft's circumferential ultimate strength was 2.57 MPa and its strain was 339%. The toe region of the ESM/TPU graft was found to be around 20% in Fig. 5 B. Compared to human blood vessels, ESM/TPU grafts have good mechanical strength, which suggests that the grafts have the ability to bear blood pressure. In Fig. 5 B, cyclic mechanical tests were performed on ESM/TPU tubes in the circumferential direction for 100 cycles. According to the experimental results, the toe region in the tensile stress–strain curve was reflected in the wavy structure, and cyclic loading showed good repeatability. At the beginning of cyclic loading, the loop was unstable. This was because of the residual stress in the scaffold. After the release of residual stress, the cyclic load loop became stable and almost coincident.

3.3. Surface Chemistry

The inner ESM was used to promote the proliferation and rapid attachment of endothelial cells. To enhance the effectiveness of endothelialization using HUVECs on the luminal ESM, a series of surface modifications were performed in this study. Dopamine was polymerized under weak alkalinity (PH 8.5) in air and coated on the ESM surface easily because of its strong adhesive behavior [51]. Polydopamine is considered a glue protein that bonds strongly to virtually all inorganic and organic surfaces. The detailed binding mechanisms between polydopamine and the ESM surface are speculated to be a reaction between the catechol/quinone groups of the polydopamine coating and the hydroxyl or carboxyl groups of the ESM to form covalent bonds. The polydopamine coating was found to be an extremely versatile platform for secondary reactions, which led to the tailoring of the coatings for diverse functional uses. Heparin could also be immobilized on the polydopamine (PDA) due to PDA's adhesive properties and the fact that the amino groups of the heparin could be covalently grafted on the phenolic hydroxyl groups of the PDA [39].

The surface morphology of the modified ESM was imaged using SEM as depicted in Fig. 6. The particulates observed on the ESM fibers were from the self-polymerized PDA that formed particles in the aqueous solution. Thus, when heparin was grafted on the PDA-ESM surface, the resulting H-PDA-ESM showed more particles anchored to the ESM fibers as heparin molecules tended to aggregate and form particles when dried from the aqueous solution [52]. The same particles were also found on ESM fibers when heparin alone was grafted on the ESM.

The chemical composition of the modified ESM was characterized by Fourier transform infrared (FTIR) spectroscopy (cf. Fig. 7). The FTIR spectrum in Fig. 7 (A) exhibited distinct peaks at 3300, 1634, 1536, and 1240 cm^{-1}, which were due to strong signals from the ESM. The peak position at 3300 cm^{-1} represented the O–H and N–H groups, which indicated that a large amount of amino acids were present in the ESM. The 1634 cm^{-1} peak indicated the C=O group, and the 1536 cm^{-1} and 1240 cm^{-1} peak represented the C–N and N–H groups,

respectively. These bonds reflected the amide I, amide II, and amide III that existed in the ESM [53].

In Fig. 7 (B), the peak that appeared at 1101 cm^{-1} demonstrated the C–O bond of the phenol group that exists in polydopamine [54]. The peak at 1280 cm^{-1} represented the C–N bond of the aniline ring, which is a functional group in polydopamine. These results indicated the successful coating of dopamine on the PDA-ESM. When heparin was further grafted onto the H-PDA-ESM surface, a shoulder peak assigned to the S=O asymmetric vibration appeared on the FTIR spectrum at 1018 cm^{-1}, which was the obvious chemical bond of heparin (cf. Fig. 7 (B)) [55][56]. Also the characteristic adsorption at 1030 cm^{-1} ($-SO_3^-$) occurred in the spectrum, which indicated the existence of heparin on the H-PDA-ESM [57].

3.4. HUVEC Viability and Proliferation

This study focused on improving the biological properties of ESM/TPU grafts with surface-modified ESM for HUVEC rapid adhesion and proliferation. The modified ESM fibrous network was beneficial for endothelial cell growth and helped the vascular grafts achieve rapid endothelialization [58–60]. The initial cell attachment experiment was evaluated on TPU, ESM, PDA-ESM, H-ESM, and H-PDA-ESM samples. It was found that the cell attachment on the modified ESM samples was significantly better than on the TPU samples.

Figure 8 shows the proliferation of HUVECs on ESM/TPU grafts with differently modified ESM surfaces after an incubation time of 1, 3, and 7 days. The live/dead viability kit was used, in which calcein-AM targeted live cells with green fluorescence and EthD-1 stained dead cells with red fluorescence. From the fluorescence images, the HUVECs grew differently on the different samples. Tissue culture plastic (TCP) was used as the control. After 7 days of incubation, HUVECs on all ESM samples grew faster than on the TPU sample. This was due to the high hydrophobicity of TPU, such that the TPU sample had low cell adhesion and could not be endothelialized. Since ESM is a naturally hydrophilic biomaterial, it is more suitable for cell growth than TPU. The effect of PDA and heparin on cell growth was also compared. HUVECs on PDA-ESM and H-ESM proliferated well and distributed evenly after 7 days of culture and no obvious difference was seen between them.

To verify the fluorescence staining results, a Cell Counting Kit-8 (CCK-8) was used to quantify cell proliferation (Fig. 9). As time passed, the cell viability on all samples increased. The cell viability on TPU samples was the lowest and grew slowly, while the cell viability on TCP was the highest and grew quickly. Comparing the PDA- and heparin-modified ESM with the original ESM, PDA-ESM and H-ESM had higher cell viabilities than the original ESM. The cell viabilities of PDA-ESM and H-ESM were almost the same. CCK-8 test results agreed well with the live and dead test results. Heparin was shown to promote endothelial cell growth by facilitating their interaction with cell surface receptors [61,62]. PDA-ESM samples showed improved cell viability, mainly due to native serum proteins that were adhered on the dopamine surface. The serum proteins interacted with the cell membrane adhesion receptors; thus, PDA had better adhesive properties for cells [55,63,64].

3.5. HUVEC Cytoskeleton and Morphology

To observe cell morphology, the cell cytoskeletons were stained red with phalloidin while the cell nuclei were stained blue with 4', 6-diamidino-2-phenylindole (DAPI). The HUVECs were cultured on ESM, PDA-ESM, H-ESM, H-PDA-ESM, and TPU samples for 7 days, with TCP as the control.

From Fig. 10, it can be seen that the cells on the TPU sample grew slower than the other groups, while the cells cultured on different ESM samples showed a healthy growing state and a clear cell profile. After PDA and heparin modification, whether on PDA-ESM, H-ESM, or H-PDA-ESM, all samples had more cells than on the original ESM. These results were similar for the live and dead and CCK-8 assays. The cells cultured on modified ESM surfaces spread out and stretched well. Also, the cells showed a typical spindle-like morphology and filopodia with extremely flourishing growing states. In some regions of the H-ESM and H-PDA-ESM samples, cells started to grow on top of each other and interconnected to form dense cell aggregates. This was mainly attributed to the PDA and heparin, which promoted cell attachment and spreading by interacting with cell membranes.

All of these results strongly suggest that ESM had better biocompatibility than TPU, and PDA and heparin grafting on ESM greatly improved the cell attachment of HUVECs.

In order to study the interactions between cells and substrates in detail, the cell-cultured samples at day 7 were imaged using SEM to observe their cellular morphology on the different substrates. From Fig. 11, it can be seen that the cell membranes were greatly flattened and tightly adhered to the substrates. Some cell boundaries were clear and many cells were fully spread out. Many cells were also connected to each other by extended filopodia. The lamellipodia and filopodia were tightly attached to the membrane fiber, and at the dense cell aggregate regions, the boundaries of the cell membranes overlapped and were difficult to see. These results clearly suggest strong cellular–substrate interactions.

3.6. Platelet Adhesion

Apart from rapid endothelialization, antithrombosis is another important issue for the implantation of vascular grafts [65]. The human body has a normal rejection reaction to foreign grafts. The artificial grafts need proper modification otherwise they cause thrombosis. A platelet adhesion assay was performed to characterize the effect of surface modification on the risk of thrombosis. If the platelets easily attach or aggregate on the surface, the material will be considered thrombogenic [66].

As shown in Fig. 12, the morphologies of the platelets adhered on the ESM, PDA-ESM, H-ESM, and H-PDA-ESM surfaces were examined by SEM to study the thrombogenicity of the modified sample surfaces. Many platelets were found on the ESM and PDA-ESM surfaces. In addition, platelets on the ESM and PDA-ESM surfaces were pseudopodial and aggregated. From Fig. 12 (F), PDA-ESM had more thrombogenic behavior than the original ESM due to PDA's adhesiveness. These observations indicate that the ESM and PDA-ESM surfaces were thrombogenic. The number of attached platelets on the H-ESM and H-PDA-ESM was significantly less than on the ESM and PDA-ESM. Platelets seldom adhered to H-ESM and H-PDA-ESM, suggesting improved hemocompatibility. This very low platelet

adhesion was mainly attributed to the introduction of heparin, which is a very effective anticoagulant due to its high negative charge density [37,67]. These platelet adhesion results suggest that H-ESM and H-PDA-ESM promoted the adhesion and growth of HUVECs, while successfully inhibiting the attachment of platelets.

4. Conclusions

Double-layer, small-diameter vascular grafts made of an inner eggshell membrane (ESM) and an outer TPU layer were successfully fabricated using a wavy cross-section rotating collector in an electrospinning process. The inner layer of avian ESM was comprised of abundant collagens and amino acids. This unique and natural biomaterial was used in conjunction with an outer TPU layer fabricated by electrospinning to create double-layer, small-diameter grafts. The TPU not only showed a fibrous morphology, it also supported the ESM and had good mechanical strength. The nonlinear mechanical behavior in the tensile stress–strain curve was made possible by the wavy structure, and cyclic loading showed good graft repeatability. The ESM/TPU graft could expand and contract repeatedly, and the wavy cross-section effectively helped the graft have biomimetic mechanical properties during loading and unloading, without affecting its mechanical strength or properties.

In vitro HUVEC cultures revealed that modified ESM samples (i.e., samples with a coating of polydopamine and heparin) had better biocompatibility than the TPU sample. Thus, modified ESM used as vascular intima was a good choice for cell affinity and encouraged rapid endothelialization. Bioactive molecules, including polydopamine (PDA) and heparin, were applied and successfully coated on the ESM, which was verified via FTIR and SEM. PDA-ESM, H-ESM, and H-PDA-ESM had a positive effect compared to the original ESM sample. The cell viability and proliferation all improved on the modified ESM samples. HUVECs cultured on all ESM samples exhibited favorable cell morphologies and strong cell–substrate interactions. Platelet adhesion decreased dramatically when heparin was grafted onto the surface, thereby demonstrating good antithrombogenicity.

In summary, the simultaneous improvement of endothelial cell affinity, antithrombogenicity, and nonlinear mechanical characteristics was achieved with the modified ESM/TPU double-layered vascular grafts. Given their fast endothelialization potential and good mechanical properties, these small-diameter vascular grafts have the potential for use in clinical applications.

Supplementary Material

Refer to Web version on PubMed Central for supplementary material.

Acknowledgments

This research reported was partially supported by the NHLBI of the National Institutes of Health under award number U01HL134655. The content is solely the responsibility of the authors and does not necessarily represent the official views of the National Institutes of Health. Support was also provided by the Karen Thompson Medhi Professorship and the Office of the Vice Chancellor for Research and Graduate Education at the University of Wisconsin-Madison. The authors would like to thank the Wisconsin Institute for Discovery at the University of Wisconsin-Madison for the experimental lab and equipment, the National Center for International Research of Micro-Nano Molding Technology at Zhengzhou University, the International Science & Technology Cooperation

Program of China (No. 2015DFA30550), and the China Scholarship Council for their financial support (201707040014).

References

[1]. Mi H-Y, Jiang Y, Jing X, Enriquez E, Li H, Li Q, Turng L-S, Fabrication of triple-layered vascular grafts composed of silk fibers, polyacrylamide hydrogel, and polyurethane nanofibers with biomimetic mechanical properties, Mater. Sci. Eng. C 98 (2019) 241–249.

[2]. Jiang Y-C, Jiang L, Huang A, Wang X-F, Li Q, Turng L-S, Electrospun polycaprolactone/gelatin composites with enhanced cell–matrix interactions as blood vessel endothelial layer scaffolds, Mater. Sci. Eng. C 71 (2017) 901–908.

[3]. Benjamin EJ, Muntner P, Bittencourt MS, Heart disease and stroke statistics-2019 update: A report from the American Heart Association, Circulation. 139 (2019) e56–e528. [PubMed: 30700139]

[4]. Catto V, Farè S, Freddi G, Tanzi MC, Vascular tissue engineering: recent advances in small diameter blood vessel regeneration, ISRN Vasc. Med 2014 (2014).

[5]. Mozaffarian D, Benjamin EJ, Go AS, Arnett DK, Blaha MJ, Cushman M, Das SR, De Ferranti S, Després J-P, Fullerton HJ, Executive summary: heart disease and stroke statistics—2016 update: a report from the American Heart Association, Circulation. 133 (2016) 447–454. [PubMed: 26811276]

[6]. Cattaneo I, Figliuzzi M, Azzollini N, Catto V, Farè S, Tanzi MC, Alessandrino A, Freddi G, Remuzzi A, In vivo regeneration of elastic lamina on fibroin biodegradable vascular scaffold, Int. J. Artif. Organs 36 (2013) 166–174. [PubMed: 23404641]

[7]. Marelli B, Achilli M, Alessandrino A, Freddi G, Tanzi MC, Farè S, Mantovani D, Collagen-Reinforced Electrospun Silk Fibroin Tubular Construct as Small Calibre Vascular Graft, Macromol. Biosci 12 (2012) 1566–1574. [PubMed: 23060093]

[8]. Ingulli E, Mechanism of cellular rejection in transplantation, Pediatr. Nephrol 25 (2010) 61. [PubMed: 21476231]

[9]. Martinu T, Pavlisko EN, Chen D-F, Palmer SM, Acute allograft rejection: cellular and humoral processes, Clin. Chest Med 32 (2011) 295–310. [PubMed: 21511091]

[10]. Mackenzie DC, Loewenthal J, Endothelial growth in nylon vascular grafts, Br. J. Surg 48 (1960) 212–217. [PubMed: 13764903]

[11]. Tapp JS, Flexible nylon tube and method for preparing same, (1958).

[12]. Kakisis JD, Antonopoulos C, Mantas G, Alexiou E, Katseni K, Sfyroeras G, Moulakakis K, Geroulakos G, Safety and efficacy of polyurethane vascular grafts for early hemodialysis access, J Vasc. Surg 66 (2017) 1792–1797. [PubMed: 28865977]

[13]. Zhu Y, Gao C, He T, Shen J, Endothelium regeneration on luminal surface of polyurethane vascular scaffold modified with diamine and covalently grafted with gelatin, Biomaterials. 25 (2004) 423–430. [PubMed: 14585690]

[14]. Isenberg BC, Williams C, Tranquillo RT, Small-diameter artificial arteries engineered in vitro, Circ. Res 98 (2006) 25–35. [PubMed: 16397155]

[15]. MacNeill BD, Pomerantseva I, Lowe HC, Oesterle SN, Vacanti JP, Toward a new blood vessel, Vasc. Med 7 (2002) 241–246. [PubMed: 12553747]

[16]. Conte MS, The ideal small arterial substitute: a search for the Holy Grail?, FASEB J. 12 (1998) 43–45. [PubMed: 9438409]

[17]. LEACH RM JR, Biochemistry of the organic matrix of the eggshell, Poult. Sci 61 (1982) 2040–2047.

[18]. Chowdhury SD, Shell membrane protein system in relation to lathyrogen toxicity and copper deficiency, Worlds. Poult. Sci. J 46 (1990) 153–169.

[19]. Kaweewong K, Garnjanagoonchorn W, Jirapakkul W, Roytrakul S, Solubilization and identification of hen eggshell membrane proteins during different times of chicken embryo development using the proteomic approach, Protein J. 32 (2013) 297–308. [PubMed: 23636516]

[20]. Arias JL, Fink DJ, Xiao S-Q, Heuer AH, Caplan AI, Biomineralization and eggshells: cell-mediated acellular compartments of mineralized extracellular matrix, in: Int. Rev. Cytol, Elsevier, 1993: pp. 217–250.

[21]. Nys Y, Gautron J, Garcia-Ruiz JM, Hincke MT, Avian eggshell mineralization: biochemical and functional characterization of matrix proteins, Comptes Rendus Palevol. 3 (2004) 549–562.

[22]. Zhao Y-H, Chi Y-J, Characterization of collagen from eggshell membrane, Biotechnology. 8 (2009) 254–258.

[23]. Harris ED, Blount JE, Leach RM, Localization of lysyl oxidase in hen oviduct: implications in egg shell membrane formation and composition, Science (80–.). 208 (1980) 55–56.

[24]. Maeda K, Sasaki Y, An experience of hen-egg membrane as a biological dressing, Burns. 8 (1982) 313–316.

[25]. Tavassoli M, Effect of the substratum on the growth of CFU-c in continuous marrow culture, Experientia. 39 (1983) 411–412. [PubMed: 6832324]

[26]. Arias JI, Gonzalez A, Fernandez MS, Gonzalez C, Saez D, Arias JL, Eggshell membrane as a biodegradable bone regeneration inhibitor, J. Tissue Eng. Regen. Med 2 (2008) 228–235. [PubMed: 18493912]

[27]. Ohto-Fujita E, Konno T, Shimizu M, Ishihara K, Sugitate T, Miyake J, Yoshimura K, Taniwaki K, Sakurai T, Hasebe Y, Hydrolyzed eggshell membrane immobilized on phosphorylcholine polymer supplies extracellular matrix environment for human dermal fibroblasts, Cell Tissue Res. 345 (2011) 177–190. [PubMed: 21597915]

[28]. Baláž M, Eggshell membrane biomaterial as a platform for applications in materials science, Acta Biomater. 10 (2014) 3827–3843. [PubMed: 24681370]

[29]. Jia J, Liu G, Yu J, Duan Y, Preparation and characterization of soluble eggshell membrane protein/PLGA electrospun nanofibers for guided tissue regeneration membrane, J. Nanomater 2012 (2012) 25.

[30]. Ruff KJ, Endres JR, Clewell AE, Szabo JR, Schauss AG, Safety evaluation of a natural eggshell membrane-derived product, Food Chem. Toxicol 50 (2012) 604–611. [PubMed: 22245377]

[31]. Ruff KJ, DeVore DP, Leu MD, Robinson MA, Eggshell membrane: a possible new natural therapeutic for joint and connective tissue disorders. Results from two open-label human clinical studies, Clin. Interv. Aging 4 (2009) 235. [PubMed: 19554094]

[32]. Bayati V, Altomare L, Tanzi MC, Fare S, Adipose-derived stem cells could sense the nano-scale cues as myogenic-differentiating factors, J. Mater. Sci. Mater. Med 24 (2013) 2439–2447. [PubMed: 23793565]

[33]. Caracciolo PC, Rial-Hermida MI, Montini-Ballarin F, Abraham GA, Concheiro A, Alvarez-Lorenzo C, Surface-modified bioresorbable electrospun scaffolds for improving hemocompatibility of vascular grafts, Mater. Sci. Eng. C 75 (2017) 1115–1127.

[34]. Montini-Ballarin F, Calvo D, Caracciolo PC, Rojo F, Frontini PM, Abraham GA, V Guinea G, Mechanical behavior of bilayered small-diameter nanofibrous structures as biomimetic vascular grafts, J. Mech. Behav. Biomed. Mater 60 (2016) 220–233. [PubMed: 26872337]

[35]. Marcolin C, Draghi L, Tanzi M, Faré S, Electrospun silk fibroin–gelatin composite tubular matrices as scaffolds for small diameter blood vessel regeneration, J. Mater. Sci. Mater. Med 28 (2017) 80. [PubMed: 28397163]

[36]. Catto V, Farè S, Cattaneo I, Figliuzzi M, Alessandrino A, Freddi G, Remuzzi A, Tanzi MC, Small diameter electrospun silk fibroin vascular grafts: Mechanical properties, in vitro biodegradability, and in vivo biocompatibility, Mater. Sci. Eng. C 54 (2015) 101–111.

[37]. Yao Y, Wang J, Cui Y, Xu R, Wang Z, Zhang J, Wang K, Li Y, Zhao Q, Kong D, Effect of sustained heparin release from PCL/chitosan hybrid small-diameter vascular grafts on anti-thrombogenic property and endothelialization, Acta Biomater. 10 (2014) 2739–2749. [PubMed: 24602806]

[38]. Yu E, Mi H, Zhang J, Thomson JA, Turng L, Development of biomimetic thermoplastic polyurethane/fibroin small-diameter vascular grafts via a novel electrospinning approach, J. Biomed. Mater. Res. Part A 106 (2018) 985–996.

[39]. Gao A, Liu F, Xue L, Preparation and evaluation of heparin-immobilized poly (lactic acid)(PLA) membrane for hemodialysis, J. Memb. Sci 452 (2014) 390–399.

[40]. Lee H, Scherer NF, Messersmith PB, Single-molecule mechanics of mussel adhesion, Proc. Natl. Acad. Sci 103 (2006) 12999–13003. [PubMed: 16920796]

[41]. Lee H, Dellatore SM, Miller WM, Messersmith PB, Mussel-inspired surface chemistry for multifunctional coatings, Science (80-.). 318 (2007) 426–430.

[42]. Singh C, Wong C, Wang X, Medical textiles as vascular implants and their success to mimic natural arteries, J. Funct. Biomater 6 (2015) 500–525. [PubMed: 26133386]

[43]. Burton AC, Relation of structure to function of the tissues of the wall of blood vessels, Physiol. Rev 34 (1954) 619–642. [PubMed: 13215088]

[44]. Kochová P, Kuncová J, Švíglerová J, Cimrman R, Miklíková M, Liška V, Tonar Z, The contribution of vascular smooth muscle, elastin and collagen on the passive mechanics of porcine carotid arteries, Physiol. Meas 33 (2012) 1335. [PubMed: 22813960]

[45]. Kielty CM, Stephan S, Sherratt MJ, Williamson M, Shuttleworth CA, Applying elastic fibre biology in vascular tissue engineering, Philos. Trans. R. Soc. B Biol. Sci 362 (2007) 1293–1312.

[46]. Bergmeister H, Seyidova N, Schreiber C, Strobl M, Grasl C, Walter I, Messner B, Baudis S, Fröhlich S, Marchetti-Deschmann M, Biodegradable, thermoplastic polyurethane grafts for small diameter vascular replacements, Acta Biomater. 11 (2015) 104–113. [PubMed: 25218664]

[47]. Bellairs R, Boyde A, Scanning electron microscopy of the shell membranes of the hen's egg, Cell Tissue Res. 96 (1969) 237–249.

[48]. Wong Liong JW, Frank JF, Bailey S, Visualization of eggshell membranes and their interaction with Salmonella enteritidis using confocal scanning laser microscopy, J. Food Prot 60 (1997) 1022–1028. [PubMed: 31207844]

[49]. Van Andel CJ, V Pistecky P, Borst C, Mechanical properties of porcine and human arteries: implications for coronary anastomotic connectors, Ann. Thorac. Surg 76 (2003) 58–64. [PubMed: 12842513]

[50]. Hamedani BA, Navidbakhsh M, Tafti HA, Comparison between mechanical properties of human saphenous vein and umbilical vein, Biomed. Eng. Online 11 (2012) 59. [PubMed: 22917177]

[51]. Yang Z, Tu Q, Zhu Y, Luo R, Li X, Xie Y, Maitz MF, Wang J, Huang N, Mussel-Inspired Coating of Polydopamine Directs Endothelial and Smooth Muscle Cell Fate for Re-endothelialization of Vascular Devices, Adv. Healthc. Mater 1 (2012) 548–559. [PubMed: 23184789]

[52]. Cheng C, Sun S, Zhao C, Progress in heparin and heparin-like/mimicking polymer-functionalized biomedical membranes, J. Mater. Chem. B 2 (2014) 7649–7672.

[53]. Rath MK, Choi B-H, Ji M-J, Lee K-T, Eggshell-membrane-templated synthesis of hierarchically-ordered NiO–Ce0. 8Gd0. 2O1. 9 composite powders and their electrochemical performances as SOFC anodes, Ceram. Int 40 (2014) 3295–3304.

[54]. An T, Lee N, Cho H-J, Kim S, Shin D-S, Lee S-M, Ultra-selective detection of Fe 2+ ion by redox mechanism based on fluorescent polymerized dopamine derivatives, RSC Adv. 7 (2017) 30582–30587.

[55]. Mi H-Y, Jing X, Thomsom JA, Turng L-S, Promoting endothelial cell affinity and antithrombogenicity of polytetrafluoroethylene (PTFE) by mussel-inspired modification and RGD/heparin grafting, J. Mater. Chem. B 6 (2018) 3475–3485. [PubMed: 30455952]

[56]. Bogdan N, Rodríguez EM, Sanz-Rodríguez F, de la Cruz MCI, Juarranz Á, Jaque D, Solé JG, Capobianco JA, Bio-functionalization of ligand-free upconverting lanthanide doped nanoparticles for bio-imaging and cell targeting, Nanoscale. 4 (2012) 3647–3650. [PubMed: 22617960]

[57]. Gu H, Liu Y, Yin D, Cai L, Zhang B, Zhang Q, Heparin-Immobilized Polymeric Monolithic Column with Submicron Skeletons and Well-Defined Macropores for Highly Efficient Purification of Enterovirus 71, Macromol. Mater. Eng 303 (2018) 1800411.

[58]. Chen ZG, Wang PW, Wei B, Mo XM, Cui FZ, Electrospun collagen–chitosan nanofiber: A biomimetic extracellular matrix for endothelial cell and smooth muscle cell, Acta Biomater. 6 (2010) 372–382. [PubMed: 19632361]

[59]. Blakeney BA, Tambralli A, Anderson JM, Andukuri A, Lim D-J, Dean DR, Jun H-W, Cell infiltration and growth in a low density, uncompressed three-dimensional electrospun nanofibrous scaffold, Biomaterials. 32 (2011) 1583–1590. [PubMed: 21112625]

[60]. Ren X, Feng Y, Guo J, Wang H, Li Q, Yang J, Hao X, Lv J, Ma N, Li W, Surface modification and endothelialization of biomaterials as potential scaffolds for vascular tissue engineering applications, Chem. Soc. Rev 44 (2015) 5680–5742. [PubMed: 26023741]

[61]. Weatherford DA, Sackman JE, Reddick TT, Freeman MB, Stevens SL, Goldman MH, Vascular endothelial growth factor and heparin in a biologic glue promotes human aortic endothelial cell proliferation with aortic smooth muscle cell inhibition, Surgery. 120 (1996) 433–439. [PubMed: 8751615]

[62]. Soker S, Goldstaub D, Svahn CM, Vlodavsky I, Levi B-Z, Neufeld G, Variations in the size and sulfation of heparin modulate the effect of heparin on the binding of VEGF165 to its receptors, Biochem. Biophys. Res. Commun 203 (1994) 1339–1347. [PubMed: 7522446]

[63]. Ku SH, Ryu J, Hong SK, Lee H, Park CB, General functionalization route for cell adhesion on non-wetting surfaces, Biomaterials. 31 (2010) 2535–2541. [PubMed: 20061015]

[64]. Lee H, Rho J, Messersmith PB, Facile conjugation of biomolecules onto surfaces via mussel adhesive protein inspired coatings, Adv. Mater 21 (2009) 431–434. [PubMed: 19802352]

[65]. Zhang YS, Oklu R, Albadawi H, Bioengineered in vitro models of thrombosis: methods and techniques, Cardiovasc. Diagn. Ther 7 (2017) S329. [PubMed: 29399537]

[66]. Ding X, Chin W, Lee CN, Hedrick JL, Yang YY, Peptide-Functionalized Polyurethane Coatings Prepared via Grafting-To Strategy to Selectively Promote Endothelialization, Adv. Healthc. Mater 7 (2018) 1700944.

[67]. Limtiaco JFK, Jones CJ, Larive CK, Characterization of heparin impurities with HPLC-NMR using weak anion exchange chromatography, Anal. Chem 81 (2009) 10116–10123. [PubMed: 19911825]

Highlights:

- The avian eggshell membrane has the potential to yield rapid endothelialization *in vitro*.
- The heparin modification of the eggshell membrane improves its anticoagulation properties.
- The biomimetic mechanical properties of the double-layered vascular graft are provided by a wavy structure.
- The circumferentially wavy structure produced a toe region in the stress–strain.

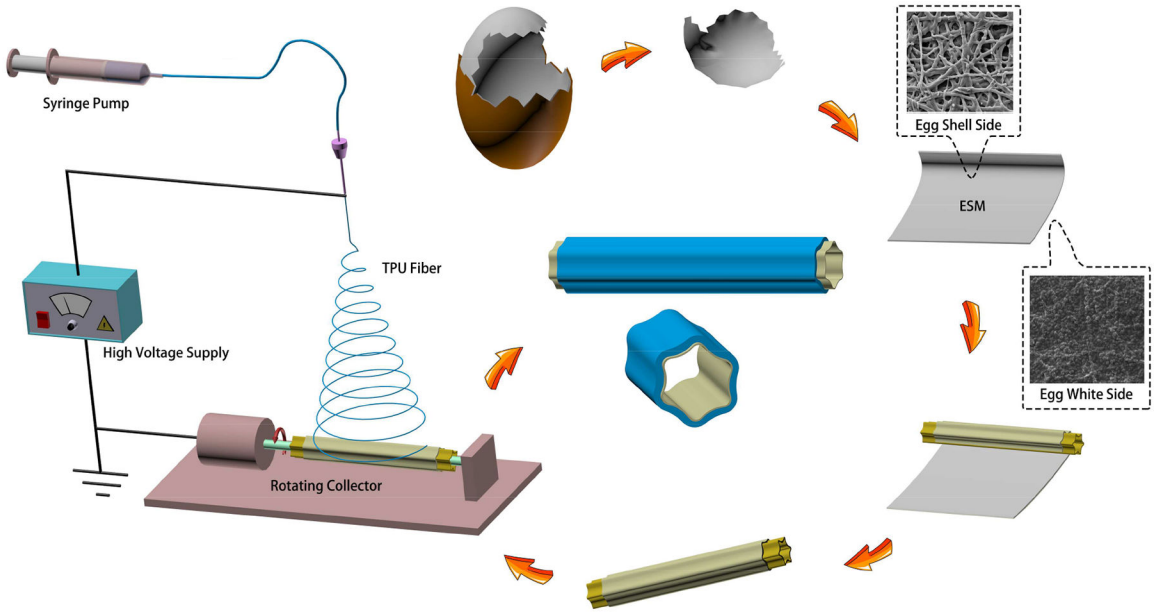

Fig. 1.
Schematic of the preparation of a double-layer ESM/TPU small-diameter vascular graft.

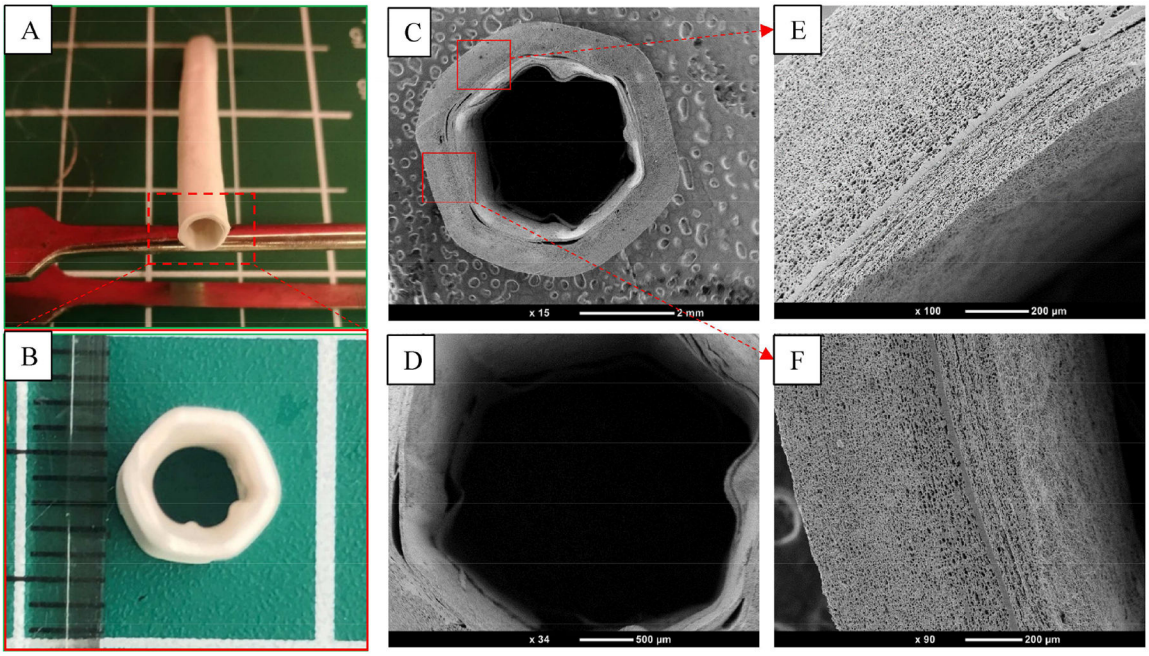

Fig. 2.

(A, B) Appearance and cross-section of an ESM/TPU small-diameter vascular graft. SEM results of (C) the cross-section of an ESM/TPU double-layered vessel. The lumen diameter of this graft was about 4 mm, and the wavy profile could be clearly seen. (D) Enlarged magnification of (C), and (E, F) the upper and lower square regions in (C), respectively.

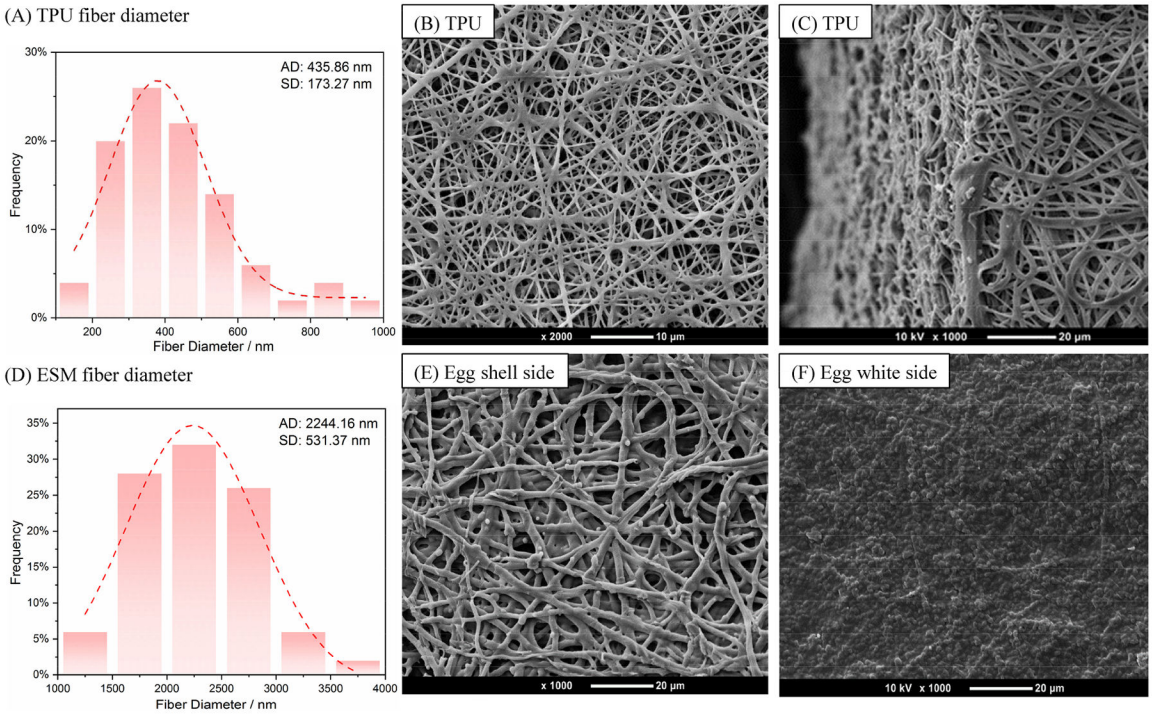

Fig. 3.

SEM results of the morphology of (A, D) TPU and ESM (shell side) diameter distribution. (B, C) Electrospun TPU membrane fibers. (E, F) ESM close to the shell side and close to the white side, respectively. ESM's shell-side surface was composed of fibers that were similar to electrospun fibers. The fibrous network encouraged EC growth and helped vascular grafts achieve rapid endothelialization. The white-side surface of the ESM had numerous rounded bulges that came into contact with the TPU membrane. (AD: average diameter; SD: standard deviation)

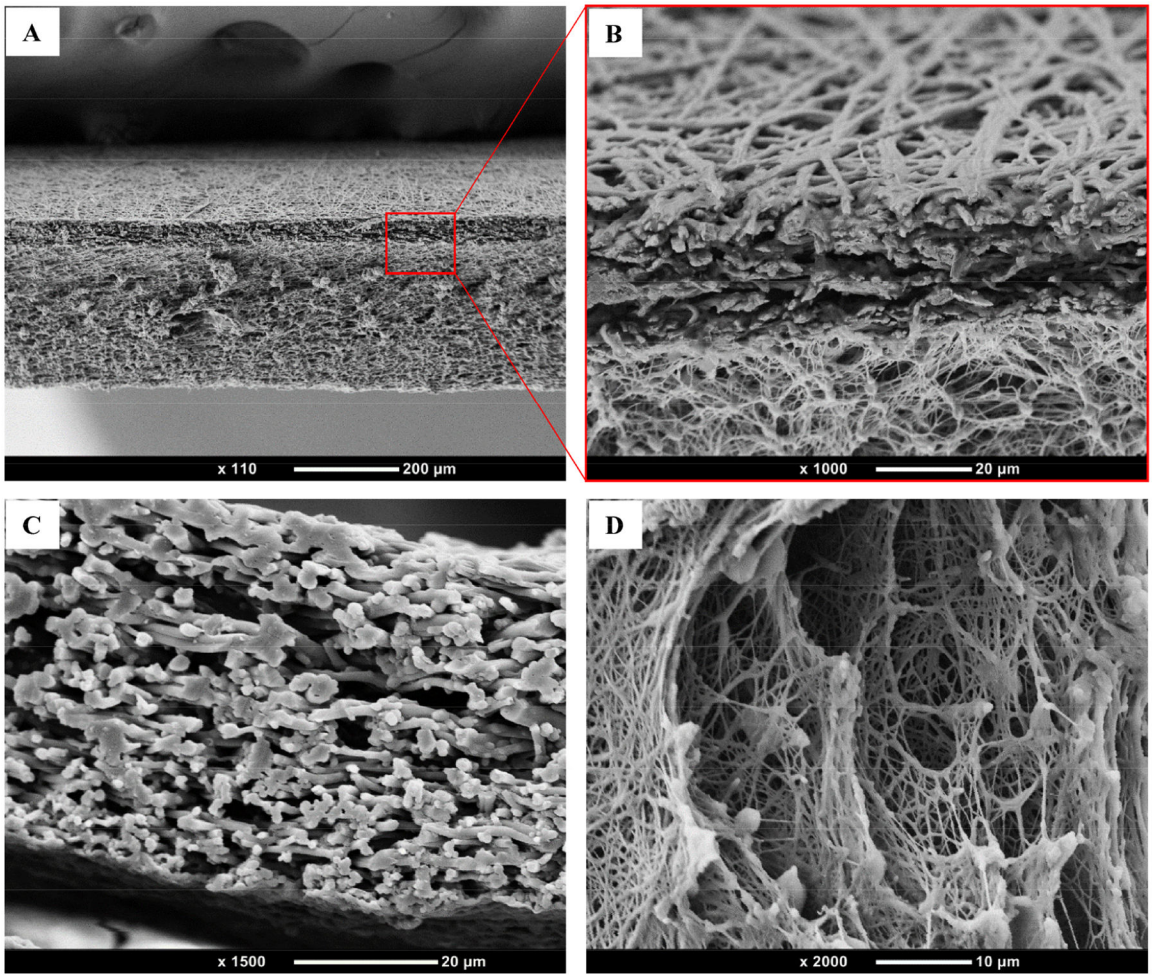

Fig. 4.

SEM results of (A) ESM/TPU double-layer cross-section, (B) enlarged magnification of (A), (C) ESM cross-section, and (D) TPU cross-section.

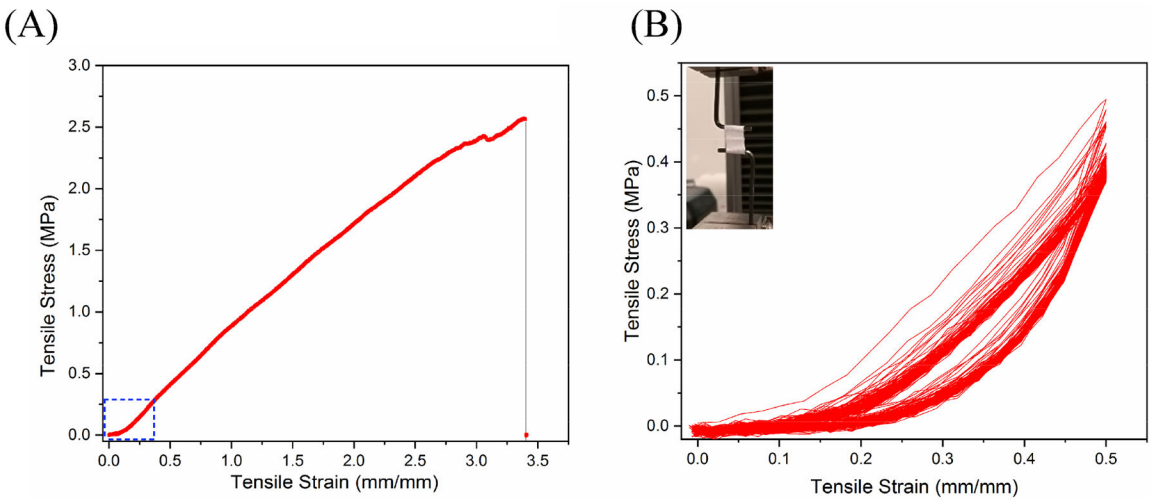

Fig. 5.

Results of (A) radial tensile tests of ESM/TPU grafts, and (B) the cyclical response of ESM/TPU grafts. The toe region in the tensile stress–strain curve was reflected in the wavy structure, and the cyclic loading showed good repeatability.

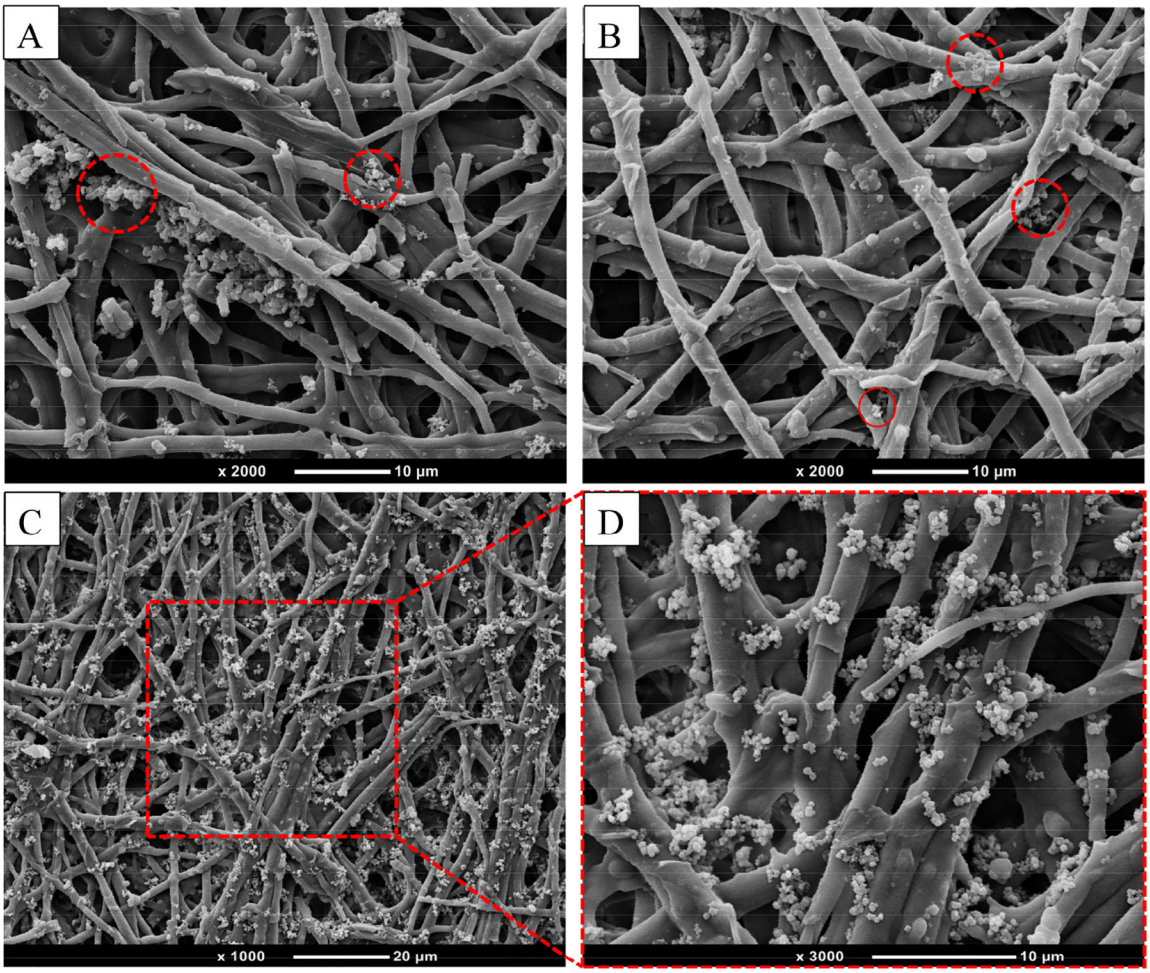

Fig. 6.

SEM images of particles grafted on ESM surfaces: (A) PDA-ESM, (B) H-ESM, (C) H-PDA-ESM, and (D) an enlarged view of the outlined region in (C).

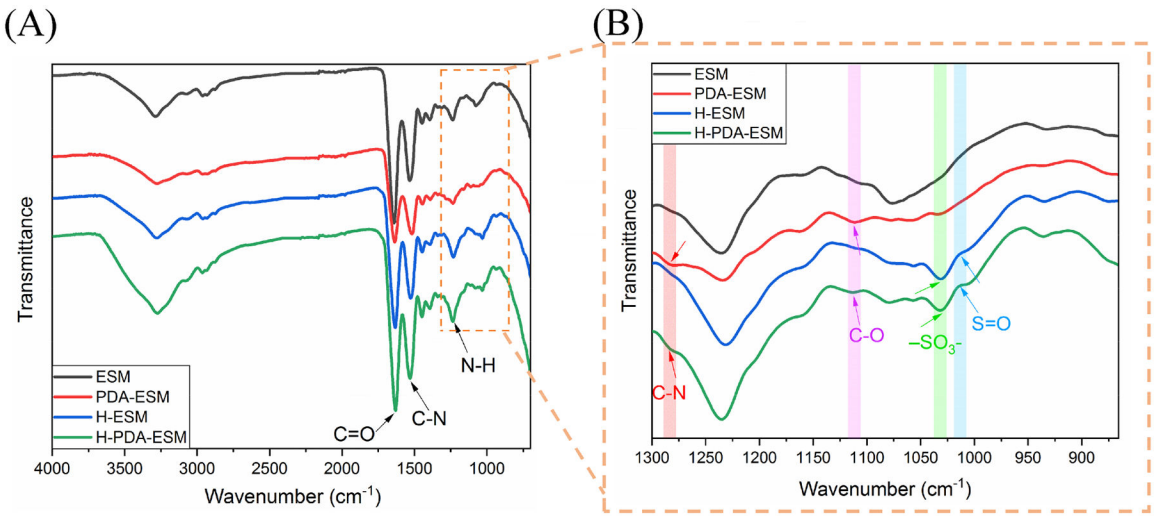

Fig. 7.
FTIR spectra of ESM, PDA-ESM, H-ESM, and H-PDA-ESM samples.

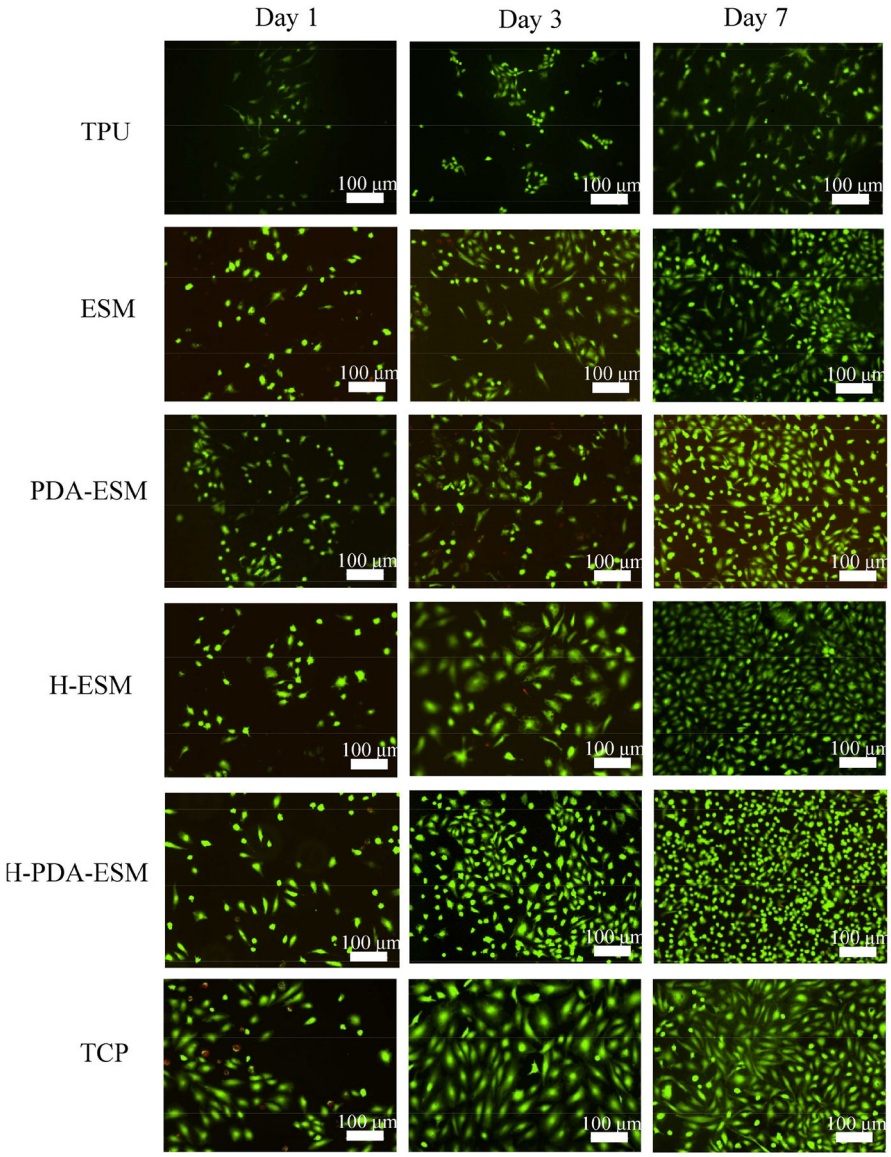

Fig. 8.

Fluorescence images of HUVECs cultured on TPU, ESM, PDA-ESM, H-ESM, H-PDA-ESM, and TCP at day 1, 3, and 7 time points.

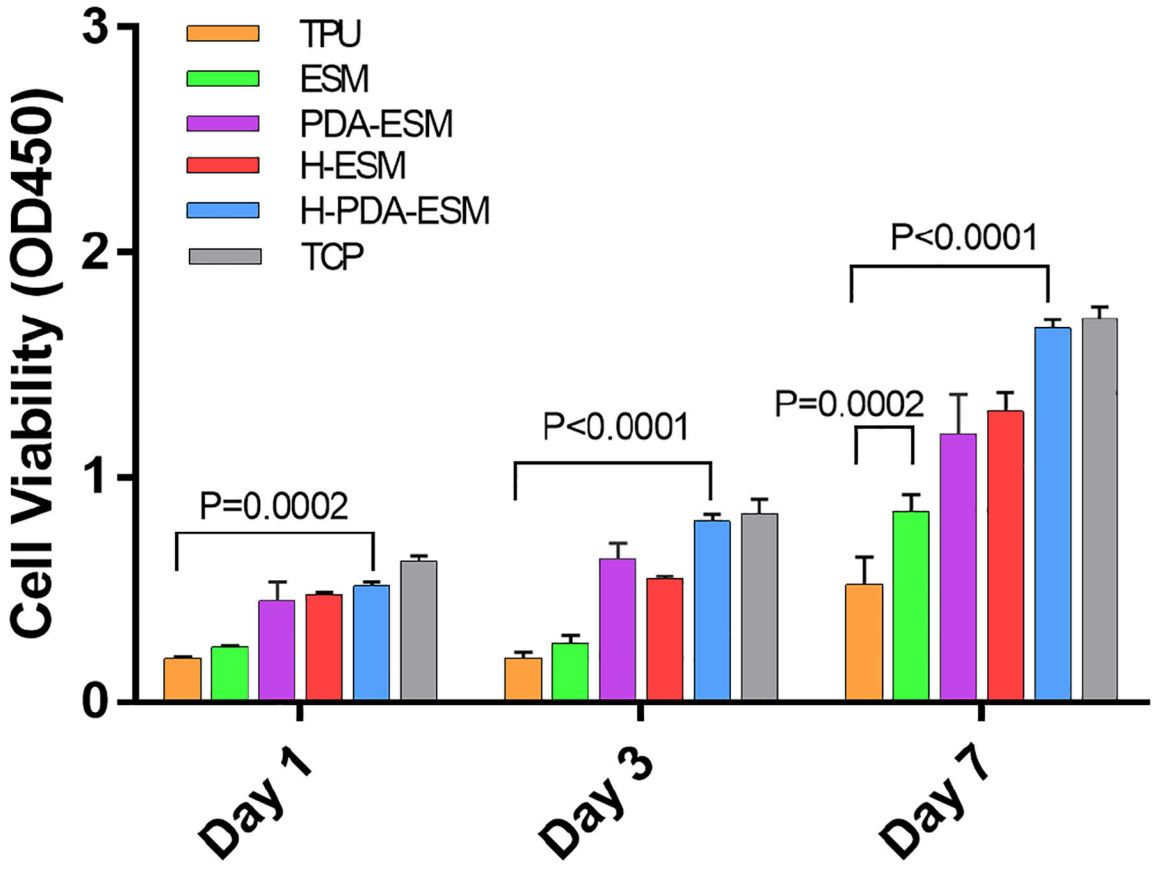

Fig. 9.
Statistical results of cell proliferation from a CCK-8 assay at day 1, 3, and 7 time points.

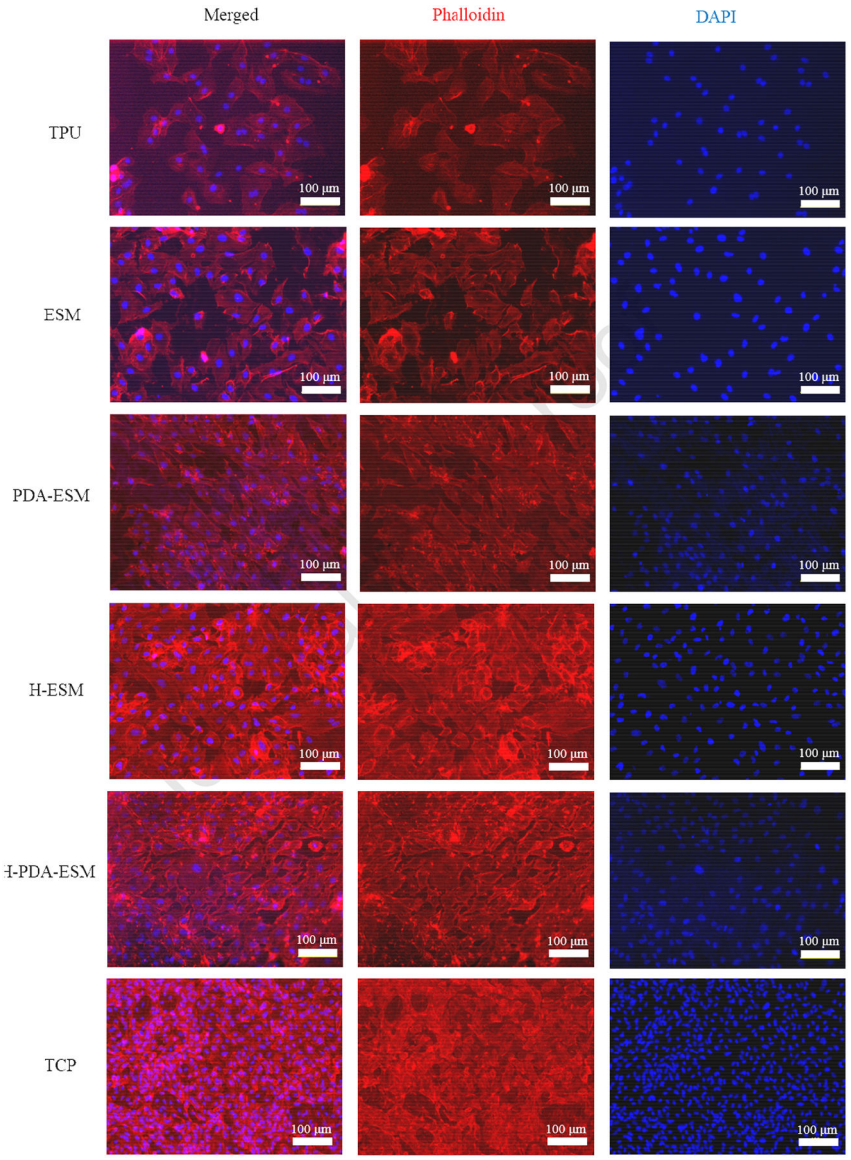

Fig. 10.

Fluorescence images showing the cytoskeleton of HUVECs cultured on TPU, ESM, PDA-ESM, H-ESM, H-PDA-ESM, and TCP for 7 days.

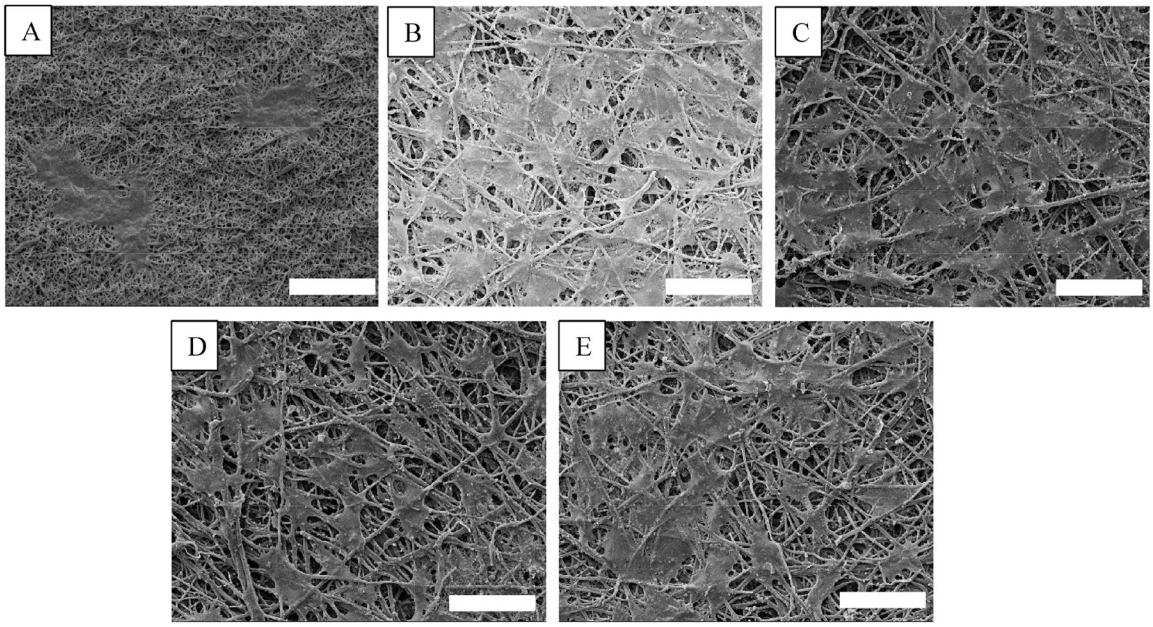

Fig. 11.

SEM images of HUVECs cultured on different ESM substrates for 7 days showing the interaction between cells and substrate: (A) TPU, (B) ESM, (C) PDA-ESM, (D) H-ESM, and (E) H-PDA-ESM. Scale bar: 50 μm.

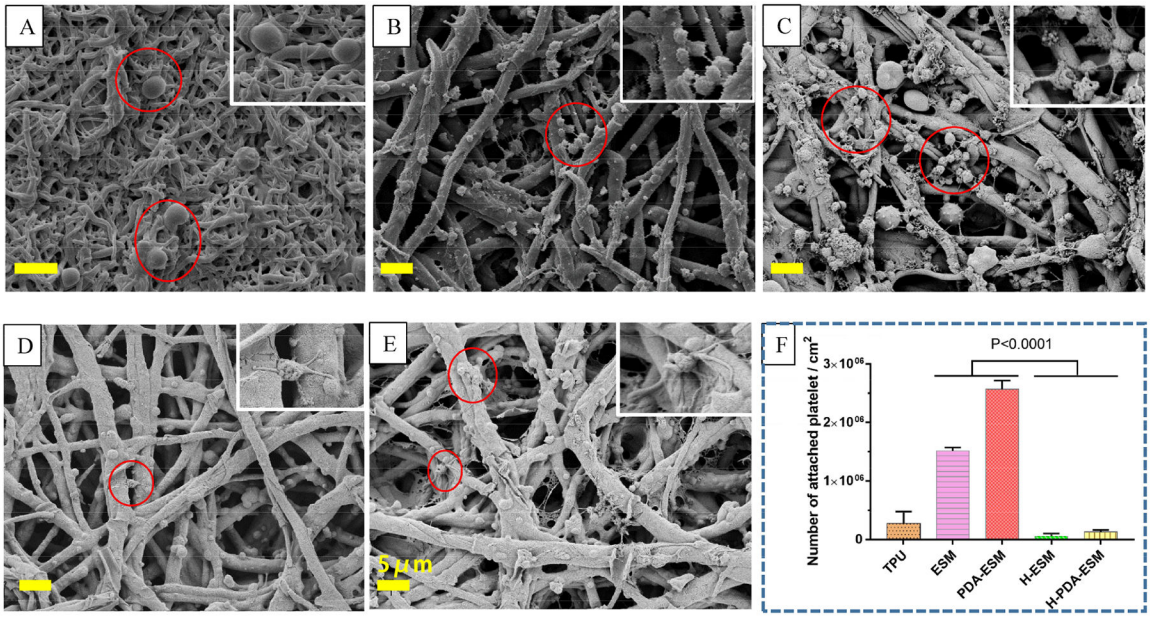

Fig. 12.

SEM images of platelet adhesion on (A) TPU, (B) ESM, (C) PDA-ESM, (D) H-ESM, and (E) H-PDA-ESM surfaces. (F) Number of attached platelets per square centimeter. Samples were incubated in platelet plasma for 2 h. (Scale bar: 5 μm.)